The Astrophysical Journal Letters, 752:L22 (5pp), 2012 June 20 doi:10.1088/2041-8205/752/2/L22

A SOLAR TORNADO OBSERVED BY AIA/*SDO*: ROTATIONAL FLOW AND EVOLUTION OF MAGNETIC HELICITY IN A PROMINENCE AND CAVITY

Xing Li[1], Huw Morgan[1,2], Drew Leonard[1], and Lauren Jeska[1]
[1] Sefydliad Mathemateg a Ffiseg, Prifysgol Aberystwyth, Ceredigion, Cymru SY23 3BZ, UK; xxl@aber.ac.uk
[2] Institute for Astronomy, University of Hawaii, 2680 Woodlawn Drive, Honolulu, HI 96822, USA
Received 2012 April 9; accepted 2012 May 15; published 2012 May 29

ABSTRACT

During 2011 September 24, as observed by the Atmospheric Imaging Assembly instrument of the *Solar Dynamic Observatory* and ground-based Hα telescopes, a prominence and associated cavity appeared above the southwest limb. On 2011 September 25 8:00 UT, material flows upward from the prominence core along a narrow loop-like structure, accompanied by a rise ($\geqslant$50,000 km) of the prominence core and the loop. As the loop fades by 10:00, small blobs and streaks of varying brightness rotate around the top part of the prominence and cavity, mimicking a cyclone. The most intense and coherent rotation lasts for over three hours, with emission in both hot ($\sim$1 MK) and cold (hydrogen and helium) lines. We suggest that the cyclonic appearance and overall evolution of the structure can be interpreted in terms of the expansion of helical structures into the cavity, and the movement of plasma along helical structures which appears as a rotation when viewed along the helix axis. The coordinated movement of material between prominence and cavity suggests that they are structurally linked. Complexity is great due to the combined effect of these actions and the line-of-sight integration through the structure which contains tangled fields.

Key words: Sun: atmosphere – Sun: corona – Sun: filaments, prominences

Online-only material: animation, color figures

1. INTRODUCTION

Filaments are highly complicated magnetic structures which lie in the lowest corona. Their structure and dynamics at small and large scales are not yet fully explained. Recent extensive reviews of their composition, structure, and dynamics are given by Labrosse et al. (2010) and Mackay et al. (2010). The relation of a filament to the surrounding magnetic structure is also complicated. Viewed above the limb, a quiescent prominence will often be situated within, or at the base of, a large system of magnetic loops. Observed in white light and in the extreme ultraviolet (EUV), a semicircular or circular region of closed loops surrounding the prominence is relatively dark compared to the surrounding corona, and is therefore labeled a coronal cavity (Waldmeier 1970; Gibson et al. 2010; Reeves et al. 2012). It has been shown, however, that cavities are not depleted of density, but are at a very high temperature on the order of 2 MK (Habbal et al. 2010). The relation between the cavity and filament is still unclear. The general filament/cavity model is of an arcade of loops anchored at the photosphere with the filament constrained within the loop system. The arcade can be raised above the photosphere in the form of a helical flux rope (Low & Hundhausen 1995).

Reports of long-lived rotation, or cyclonic, behavior of non-eruptive prominences are sporadic but have been made for a long time. Such phenomena are called "tornadoes" due to their appearance but their physics are of course very different to that of terrestrial tornadoes. Pettit (1925) describes in detail the behavior of prominences and categorize some as "tornado/spiral." Öhman (1969) measured lineshifts of Hα for filaments on the disk, and found a shift consistent with rotation of the filament at a velocity of $\sim$10 km s^{-1}. Liggett & Zirin (1984) made a study of 51 prominences and found 5 which showed rotation, with apparent velocities of 15–75 km s^{-1}, interpreted the rotation in terms of a twisting of magnetic structure, and invoked reconnection as a way to explain the long-lived rotation. Wang et al. (2010) describe the continuous rotational movement of filament cavities observed by the ExtremeUltraViolet Imaging Telescope (EIT) on board the *Solar and Heliospheric Observatory*. This movement is interpreted as a "pinch-off" of a system of arcade loops surrounding a filament, leading to a helical flux rope. Flow of material along the original arcade is then restricted to rotate around the helix.

In this Letter, we report a unique activation of a quiescent prominence observed by *Solar Dynamic Observatory* (*SDO*)/Atmospheric Imaging Assembly (AIA; Lemen et al. 2012). Such prominences are known to produce emission at temperatures to about $\log T(\mathrm{K}) \approx 5.5$ and show motions of up to 70 km s^{-1} (Wang 1999; Chae et al. 2000; Kucera et al. 2003; Kucera & Landi 2006), and upward-moving jets may be a mechanism injecting mass into prominences (Chae et al. 2000). We describe the phenomenon in detail in Section 2, and give further discussion and provide possible interpretations in Section 3.

2. OBSERVATIONS

The AIA instrument on board *SDO* measures EUV light in several narrow wavelength channels, each of which is dominated by an emission line formed at a particular temperature (Lemen et al. 2012). Its high time ($\sim$12 s) and spatial (0.″6) resolution provide a new view of the dynamics of chromospheric and coronal structures. The observations presented here are mostly of the 171 Å bandpass channel, dominated by emission of Fe^{8+} formed at $\sim$0.7 MK, and the 304 Å channel dominated by He^{1+} emission at 10^4 K (e.g., O'Dwyer et al. 2010). The filament under study is at a position angle of 215° (counterclockwise from north). Seen in Hα in a daily sequence of Big Bear Solar Observatory (BBSO) observations prior to the active phase under study, it is a nondescript filament, rather dim and ill-defined, forming part of a chain of similar filaments at the same latitude.

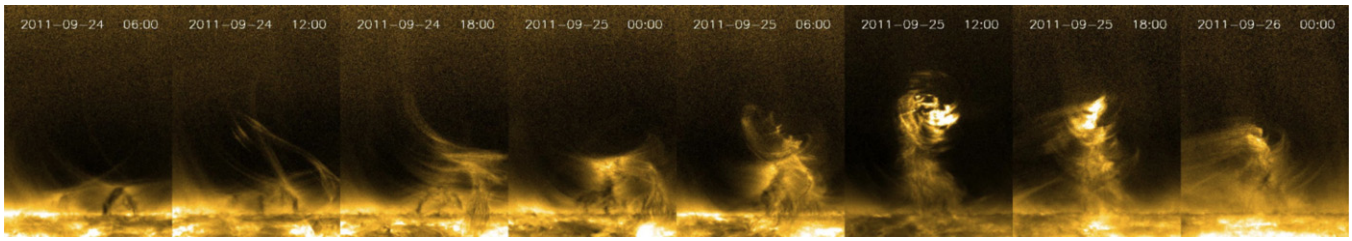

Figure 1. Development of the prominence tornado structure in the AIA 171 Å channel over almost two days, in six hour time increments from 2011 September 24 06:00 (left) to 2012 September 26 00:00 (right). These images are converted from the original images into polar coordinates, and show a section of the corona from position angle 210° to 220°, and height 0.99–1.25 $R_{\odot}$.

(A color version of this figure is available in the online journal.)

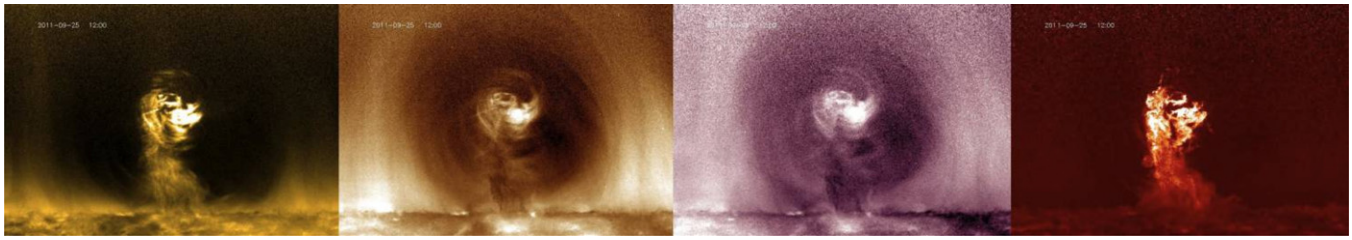

Figure 2. Different appearance of the tornado in different AIA wavelength channels at time 12:00. The main ion contributing to the signal, approximate wavelength, and approximate peak temperature sensitivity are from left to right: Fe^{8+} 171 Å (0.8 MK), Fe^{11+} 193 Å (1.5 MK), Fe^{13+} 211 Å (1.8 MK), and He^{1+}304 Å (10^4 K). The signal is too low in the other channels to warrant display.

(A color version of this figure is available in the online journal.)

Almost two days of data are analyzed from 2011 September 24 06:00 to 2011 September 26 00:00, during which time the prominence becomes active, the tornado is formed, and disappears. Figure 1 shows the development of the whole structure during this period. What is immediately apparent from this time sequence is the similarity of structure at 2011 September 24 18:00 and 2011 September 25 00:00 with other studies of filaments and their associated cavities, for example Régnier et al. (2011). The cavity is suspended above the limb, and the filament is based directly below the U-shape cradle forming the base of the cavity. The cavity is most clearly seen in the 193 Å and 211 Å channels as shown in Figure 2, which are dominated by emission lines at 1.5 and 1.8 MK, respectively. The cavity is difficult to see in the 171 Å channel, and is invisible in the 304 Å channel. Apparent in Figure 1 are dark barbs, probably components of one of the filament legs, rooted at the base of the structure from the beginning of the observation period. This configuration is consistent with the type of model described by, for example, van Ballegooijen & Martens (1989) of a large system of loops or a helix enclosing the tighter helix and cool gas of the filament itself.

From 2011 September 25 00:00 onward, the evolution of the structure is considerably different to that of Régnier et al. (2011), where an eruption of the cavity and filament was observed. Between 2011 September 25 02:30–03:10, the whole structure experiences a large-scale and short-lived wobble initially toward the pole, and small blobs are seen to appear and disappear in the cavity immediately above the filament. Accompanying this movement is a maelstrom of small-scale activity among dark fibrils at the filament base, extending upward toward the base of the cavity. By 2011 September 25 06:00 (fifth panel of Figure 1), the filament and cavity have developed a distinct tornado-like appearance, with a large circular structure atop a narrower pillar.

At ∼8:00, a significant movement of material from the main body of the filament into the cavity along a very fine channel (the width is about 3–5 pixels) is observed. By ∼8:20, more flow channels appear and the flows seem to come from both sides of the prominence. These channels rise and fall back along curved trajectories, indicating that the motions are along curved magnetic field lines. That the fine channels of flows can break into segments is possibly due to surface instabilities (Ryutova et al. 2010). The swirling motions of the channels around the prominence suggest the presence of helical magnetic fields, but it is difficult to see any helix clearly before 10:00. These motions make the prominence appear 50,000 km higher than before ∼8:00. From ∼10:00, there is a large new injection of material into the filament base from a narrow channel at one side of the filament. The upflow of this material toward the cavity base is obvious in the highest time resolution images (see online animation). The origin of the flow can be traced to a location at least 14–18 Mm above the solar limb.

Following the upflow at 10:00 and for the next ∼3 hr, there is a spectacular series of movements at the head of the tornado, with streaks and blobs of varying brightness following circular paths counterclockwise around the top of the filament pillar—what was previously a dark cavity. Figure 3 shows some still images of this action. To truly appreciate the beauty of this event, the online animation should be viewed. Blobs of material flow into space which was previously dark, highlighting magnetic structures which are otherwise invisible. At first (10:00), material is seen moving along a thin channel and by 10:10 the thin channel is already widened and a helix-like structure with at least seven turns is very obvious. The sudden appearance of a similar tightly wound helix is repeated again at about 11:00, and a less tightly wound helix is apparent at ∼11:45. The very core of the tornado head is bright and complex, with strange slow rotation and movements of filamentary structure. A bright helix can be identified in the mid-left part of the structure at 11:45, while the right part shows a more tightly wound structure. At about 12:00, a tangled helix or a group of helices at the core of the tornado head evolves in a very complicated manner. The line-of-sight (LOS) integration, and the complexity of the structure, prevents any certainty in interpreting this evolution. If there are two or more helical structures, then we would expect

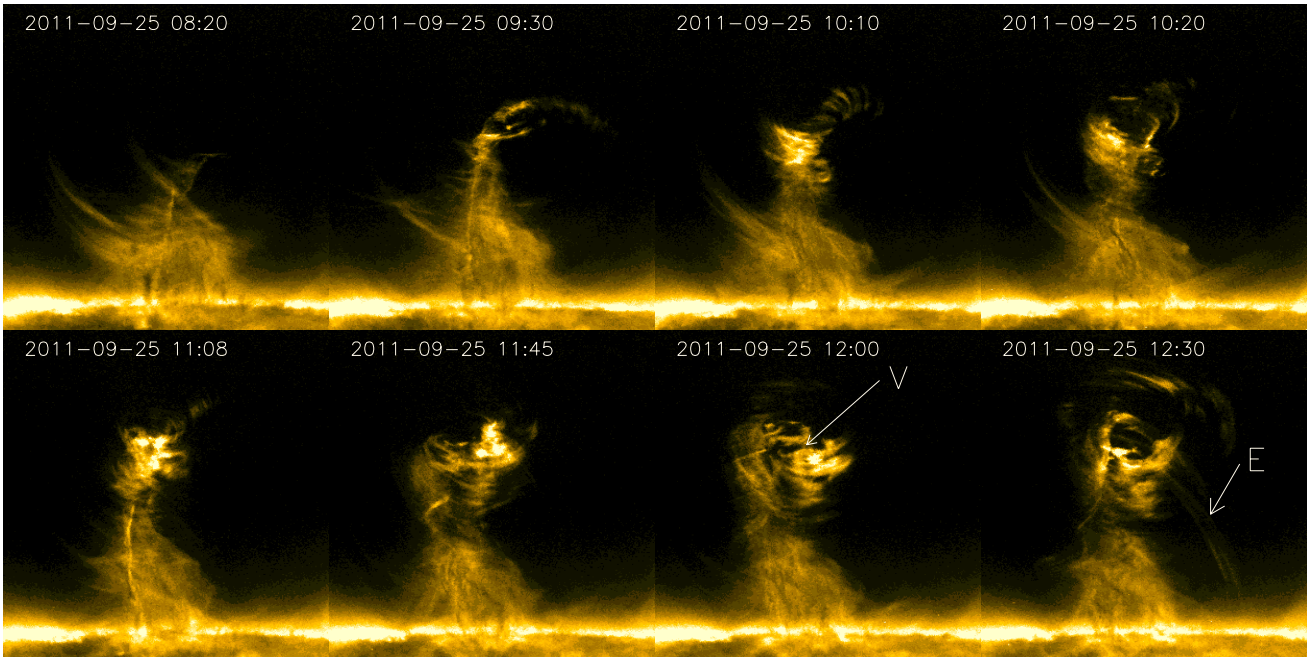

Figure 3. Evolution and rotation of the tornado as seen in the AIA 171 Å channel over ∼4 hr starting 2011 September 25 08:20 at eight different times (see the time stamps above each frame). An event in the prominence core (possibly reconnection) is labeled "V" in the frame for 12:00, followed by an ejection labeled "E" in the following frame for 12:30 (see the text).

(An animation and a color version of this figure are available in the online journal.)

some interaction–reconnection possibly, and the development of kink instabilities which may lead to entanglement of helices (Sakurai 1976). An event, possibly reconnection, is labeled "V" in Figure 3. The apparent downflows at 12:30 (labeled "E") appear to originate from the region where the bright V-shaped loop system and the loop next to it are seen to come into contact at ∼12:00 (see Figure 3). Of course, the contact could also be a projection effect.

By 18:00, the head of the tornado has dimmed, the rotational movement has stopped and by 2011 September 26 00:00 the tornado has disappeared, leaving wispy strands extending at obtuse angles relative to the radial into the region previously occupied by the filament pillar. The main period of coherent rotation lasts for approximately 3 hours.

A local correlation tracking method (Welsch et al. 2004) is adopted to compute the velocity field in the plane of the sky by using two images separated by 24 s. Two panels in Figure 4 show the velocity map at 10:09 and 12:30 with corresponding maximum speeds of 55 km s^{-1} and 95 km s^{-1}, respectively. Clear parallel arcs are seen in the higher part of the structure at 10:09. These striated patterns suggest a helical flux tube, and the direction of movement shows that the helix is expanding upward. The flow gains speed substantially, even when it ascends against gravity, suggesting that magnetic tension forces play an important role. Another possible interpretation of the striations is of density waves moving along a pre-existing helical structure. For the coherent striated patterns to be apparent, the density wave must have a wavelength close to that of the circumference of the helix windings. A detailed model study is needed to gain further understanding of this phenomenon. On top of the upward expansion of the helical structure, the rotational motion of some blobs at the top of the structure at 12:30 looks circular, and is possibly due to material flowing along helical flux tubes. As we observe along the axis of the helix, the apparent motion is rotational. Working from approximate estimates of the radius of the circular motion (about 35,000 km for a blob of material at $X = 60$, $Y = 40$), and the time for a brightness enhancement to make a complete revolution (about 3400 s), the true velocity is close to 65 km s^{-1}. This is smaller than the sound speed.

Figure 2 shows the appearance of the tornado in four AIA channels. It is not possible to assign a temperature for this structure directly since the material flowing within the structure contains ions at a large range of formation temperatures. Throughout the whole period of tornado formation and rotation, the emission in the 304 Å channel (which is dominated by emission from He^{1+}) is almost identical to that of the hotter 171 Å channel. Although the 304 Å channel can include emission from a hot line, the strength of the signal suggests that the material injected into the filament and cavity contains both hot and cold materials. The existence of cold material is also supported by the presence of Hα in the tornado structure, as shown in Figure 5. The behavior in Hα is somewhat different, although the time coverage offered by ground-based telescopes is restricted. Figure 5 shows that the tornado is emitting in Hα, but by 15:30 (last panel) the emission comes from the very base of the structure. This is different to the behavior in 304 Å emission measured by AIA, where the whole structure, including the cavity, is bright past 15:30. It is possible, therefore, that the H becomes ionized after a few hours in the top of the structure. Another factor is the sensitivity of the ground-based observations. Certainly, the BBSO observations (rightmost panel) are affected by cloud later in the day.

3. DISCUSSION AND CONCLUSION

At the start of the event, narrow helical structures are upwelling into the cavity. The exact source of these helices is unclear, although it is likely that some or all of the underlying prominence is expanding upward into the cavity possibly due to some disturbance at the prominence base. Alternatively, when a helical flux tube is tightly wound, it may be unable to maintain stability (Sakurai 1976; Hood & Priest 1979; Baty 2001) and

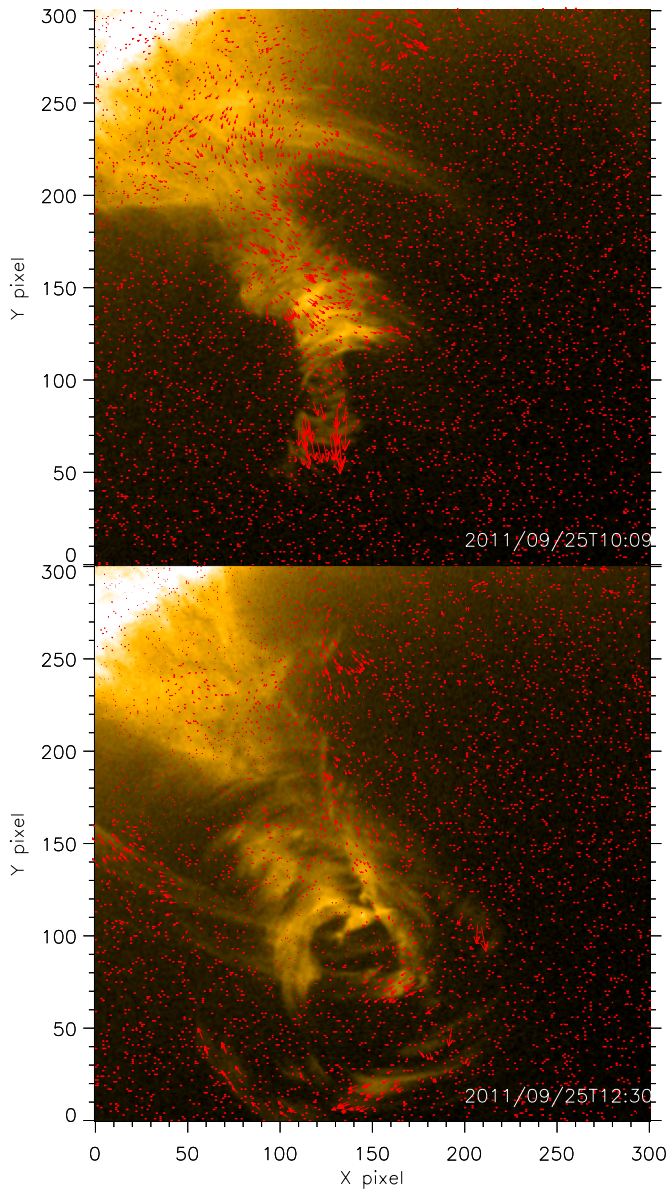

Figure 4. Apparent velocity field computed using local correlation tracking together with AIA 171 Å subfield images at 2011 September 25 10:09 (top) and 2011 September 25 12:30 (bottom) of the same prominence tornado. The maximum velocity is 55 km s^{-1} at 10:09 and 95 km s^{-1} at 12:30. The positive *Y*-axis points to the solar north.

(A color version of this figure is available in the online journal.)

may eventually expand, upwell, or untwist into the surrounding cavity without outside influence (Liggett & Zirin 1984). Following this initial development, the complex appearance and evolution of the tornado can be interpreted as a combination of several different actions. (1) The core of the tornado is formed of highly twisted magnetic fields which are unstable and interact with the surrounding cavity, possibly through reconnection. This interaction can result in sporadic localized brightenings and flows along the fields. (2) Material flows upward from the prominence base and some of this material ends up flowing along the helical fields of the prominence and/or cavity. This movement appears as a rotation when viewed along the helix axis. (3) Density waves may propagate along the helical fields. (4) There are larger-scale structural evolutions (for example, slow or rapid expansion of helices, general large-scale movements).

The filament probably consists of a highly tangled field (van Ballegooijen & Cranmer 2010), and flow within this filament will appear very complicated when the total emission is integrated over the LOS. Such embedded and kinked helices will necessarily produce favorable conditions for magnetic reconnections to occur (Baty 2000; Kwon & Chae 2008), although high twist and reconnection do not always lead to ejective behavior (Kliem et al. 2010). Reconnections may be difficult to observe in such a complex structure. The apparent downflows at 12:30 seem to originate from a region where two loop systems are seen to come into contact at ∼12:00 (see Figure 3).

Wang et al. (2010) studied rotation in coronal cavities and invoked a flow of material along an arcade of loops prior to the loops becoming detached from the solar surface and forming a helix. Their description does not seem consistent with this event, where more sporadic injections of material, and more rapid magnetic structure evolution, are observed. Although occasionally the top part of the prominence looks detached from the lower part (Figure 5 at 11:09), there is a continuous flow between the two parts and the upper part is not physically detached from the lower part of the prominence. Whether there is a preference for equatorward rotation in such tornado-like events, as suggested by Wang et al. (2010), is a matter for further observational study. If there is such a trend, then there must be a preferential direction to filament/cavity helicity and a preferential direction for material flow along the structure.

Although the flow originates from a channel 14–18 Mm above the solar limb with its width ⩽4 Mm, circular motions as wide as 90 Mm are observed at about 1.2 $R_{\odot}$, not much smaller than the diameter of the cavity (roughly 110–130 Mm from images of 193 Å). Observations of the large circular motions and flows

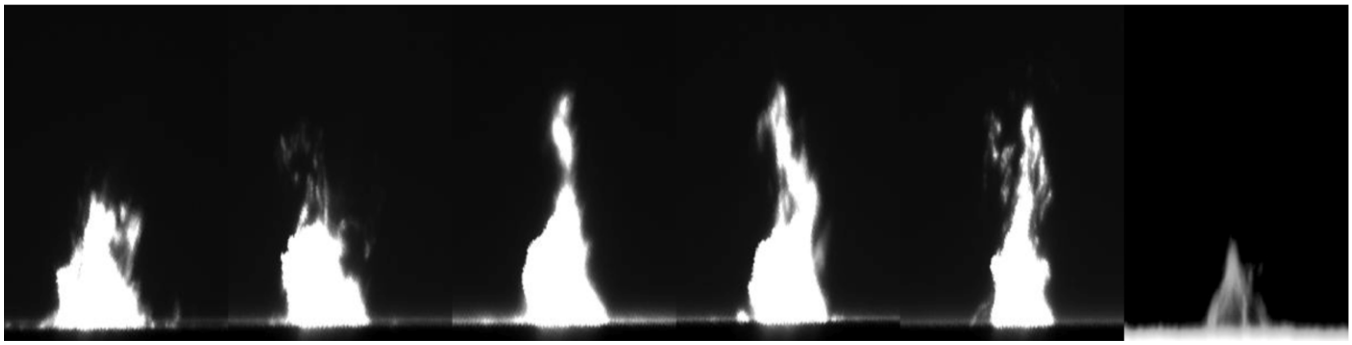

Figure 5. Tornado as observed by ground-based Hα telescopes. Panels show times 07:21, 08:57, 11:09, 11:32, 13:33, 15:30 (left to right). The observations are made by the Pic du Midi Hα coronagraph except for the rightmost panel, which is made by the Big Bear Solar Observatory (see acknowledgments).

originating from a narrow channel may shed some light on the question why a cavity exists above a prominence. If most of the magnetic field flux in the cavity is rooted in a small region in the lower atmosphere, then the small region may be simply unable to supply sufficient material into the cavity unless a dramatic injection of material is caused by some catastrophic event at the prominence base. The general (quiescent) case would therefore be of a dark cavity devoid of plasma due to the restrictive geometry of the flux tube at low heights.

The dynamics and shape of this prominence and cavity are significantly more complex than those of the erupting prominence reported by Kurokawa et al. (1987), rotational spicules reported by Pike & Mason (1998), helical "EUV sprays" reported by Harrison et al. (2001), and the emerging helical prominence reported by Okamoto et al. (2010). The prominence is several times higher than the emerging cool column reported by Okamoto et al. (2010), the flow is also a few times faster and the rotation is more coherent. The fact that the prominence reported in this Letter contains plasmas at both cool (10^4 K) and hot coronal temperatures while the emerging prominence reported by Okamoto et al. (2010) is quite cool (at $\sim 10^4$ K) suggests that the mechanisms which drive the flows in the two events may be different. Recently, Berger et al. (2011) discovered coronal-temperature plasma bubbles being injected into coronal cavities from below. Although the bubbles are small compared to cavities, they argue that the discovery offers an explanation for the 8–10 km s^{-1} flows observed by Doppler velocity measurements in cavities (Schmit et al. 2009). Such quiescent prominence convection is a more gradual and consistent process than the dynamical event described here, although it is possible that the gradual build-up of plasma, magnetic flux, and helicity to the cavity contributed to destabilization.

This huge tornado-like structure is complex and is a compelling case for further study. Similar dynamic events associated with a prominence and cavity are usually expected to erupt as a coronal mass ejection. This structure does not erupt, and remains dynamically coherent for several hours. It is therefore an interesting event which may shed light on the relationship between prominences and cavities, the evolution of helical fields in the low corona, the movement of material within cavities, the limits on magnetic structural stability prior to eruption, and the general structural characteristics of cavities. Observations of such dynamical events by AIA/*SDO* are placing new challenges to interpretation and models, and will lead to a deeper understanding of the solar atmosphere.

We are grateful to an anonymous referee for very constructive comments. The data used are provided courtesy of NASA/*SDO* and the AIA science team. Images provided by the Pic du Midi Hα coronagraph via the L'Observatoire de Paris's Bass2000 online database, and the Big Bear Solar Observatory/New Jersey Institute of Technology have been used. This work is conducted under an STFC grant to the Solar System Physics group at Aberystwyth University.

REFERENCES

Baty, H. 2000, A&A, 360, 345
Baty, H. 2001, A&A, 367, 321
Berger, T., Testa, P., Hillier, A., et al. 2011, Nature, 472, 197
Chae, J., Denker, C., Spirock, T. J., Wang, H., & Goode, P. R. 2000, Sol. Phys., 195, 333
Chae, J., Wang, H., Qiu, J., Goode, P. R., & Wilhelm, K. 2000, ApJ, 533, 535
Gibson, S. E., Kucera, T. A., Rastawicki, D., et al. 2010, ApJ, 724, 1133
Habbal, S. R., Druckmüller, M., Morgan, H., et al. 2010, ApJ, 719, 1362
Harrison, R. A., Bryans, P., & Bingham, R. 2001, A&A, 379, 324
Hood, A. W., & Priest, E. R. 1979, Sol. Phys., 64, 303
Kliem, B., Linton, M. G., Török, T., & Karlický, M. 2010, Sol. Phys., 266, 91
Kucera, T. A., & Landi, E. 2006, ApJ, 645, 1525
Kucera, T. A., Tovar, M., & de Pontieu, B. 2003, Sol. Phys., 212, 81
Kurokawa, H., Hanaoka, Y., Shibata, K., & Uchida, Y. 1987, Sol. Phys., 108, 251
Kwon, R. Y., & Chae, J. 2008, ApJ, 677, L141
Labrosse, N., Heinzel, P., Vial, J.-C., et al. 2010, Space Sci. Rev., 151, 243
Lemen, J. R., Title, A. M., Akin, D. J., et al. 2012, Sol. Phys., 275, 17
Liggett, M., & Zirin, H. 1984, Sol. Phys., 91, 259
Low, B. C., & Hundhausen, J. R. 1995, ApJ, 443, 818
Mackay, D. H., Karpen, J. T., Ballester, J. L., Schmieder, B., & Aulanier, G. 2010, Space Sci. Rev., 151, 333
O'Dwyer, B., Del Zanna, G., Mason, H. E., Weber, M. A., & Tripathi, D. 2010, A&A, 521, A21
Öhman, Y. 1969, Sol. Phys., 9, 427
Okamoto, T. J., Tsuneta, S., & Berger, T. E. 2010, ApJ, 719, 583
Pettit, E. 1925, Publ. Yerkes Obs., 3, 4
Pike, C. D., & Mason, H. E. 1998, Sol. Phys., 182, 333
Reeves, K. K., Gibson, S. E., Kucera, T. A., Hudson, H. S., & Kano, R. 2012, ApJ, 746, 146
Régnier, S., Walsh, R. W., & Alexander, C. E. 2011, A&A, 533, L1
Ryutova, M., Berger, T., Frank, Z., Tarbell, T., & Title, A. 2010, Sol. Phys., 267, 75
Sakurai, T. 1976, PASJ, 28, 177
Schmit, D. J., Gibson, S. E., Tomczyk, S., et al. 2009, ApJ, 700, L96
van Ballegooijen, A. A., & Cranmer, S. R. 2010, ApJ, 711, 164
van Ballegooijen, A. A., & Martens, P. C. H. 1989, ApJ, 343, 971
Waldmeier, M. 1970, Sol. Phys., 15, 167
Wang, Y., Cao, H., Chen, J., et al. 2010, ApJ, 717, 973
Wang, Y.-M. 1999, ApJ, 520, L71
Welsch, B., Fisher, G., Abbett, W., & Regnier, S. 2004, ApJ, 610, 1148